



## Supplemental Material

© Copyright 2018 American Meteorological Society

Permission to use figures, tables, and brief excerpts from this work in scientific and educational works is hereby granted provided that the source is acknowledged. Any use of material in this work that is determined to be “fair use” under Section 107 of the U.S. Copyright Act or that satisfies the conditions specified in Section 108 of the U.S. Copyright Act (17 USC §108) does not require the AMS’s permission. Republication, systematic reproduction, posting in electronic form, such as on a website or in a searchable database, or other uses of this material, except as exempted by the above statement, requires written permission or a license from the AMS. All AMS journals and monograph publications are registered with the Copyright Clearance Center (<http://www.copyright.com>). Questions about permission to use materials for which AMS holds the copyright can also be directed to [permissions@ametsoc.org](mailto:permissions@ametsoc.org). Additional details are provided in the AMS Copyright Policy statement, available on the AMS website (<http://www.ametsoc.org/CopyrightInformation>).

**Evaluation of CMIP5 Earth System Models for the Spatial Patterns of Biomass and Soil****Carbon Turnover Times and Their Linkage with Climate**

Donghai Wu<sup>1</sup>, Shilong Piao<sup>1,\*</sup>, Yongwen Liu<sup>1</sup>, Philippe Ciais<sup>2</sup>, and Yitong Yao<sup>1</sup>

<sup>1</sup> Sino-French Institute for Earth System Science, College of Urban and Environmental Sciences, Peking University, Beijing 100871, China.

<sup>2</sup> Laboratoire des Sciences du Climat et de l'Environnement (LSCE), CEA CNRS UVSQ, 91191 Gif Sur Yvette, France.

*\* Corresponding author address:* Shilong Piao, Sino-French Institute for Earth System Science, College of Urban and Environmental Sciences, Peking University, No.5 Yiheyuan Road Haidian District, Beijing 100871, China. E-mail: [slpiao@pku.edu.cn](mailto:slpiao@pku.edu.cn)

**Contents of this file**

Table S1

Figure S1-S19

## Introduction

This supplementary materials provide additional information mainly regarding the spatial patterns of biomass and soil carbon turnover time derived with models, spatial sensitivity of modeled biomass and soil carbon turnover time to temperature (T) and precipitation (P), and uncertainty analysis, including comparing carbon turnover time results using other data sources, and verifying the steady state assumption with CMIP5 outputs.

**Table S1** Summary of CMIP5 ESMs used in this study, including model name, coupled atmosphere model, coupled land model, nitrogen cycle (N), land use change (LUC) and fire.

**Figure S1** Global biome map constructed from the Moderate Resolution Imaging Spectroradiometer (MODIS) International Geosphere-Biosphere Program (IGBP) land-cover map referred to Todd-Brown et al. (2013).

**Figure S2** Spatial patterns of biomass carbon turnover time derived with models. Areas with no biomass (mean annual NDVI below 0.1) are masked with grey.

**Figure S3** Spatial patterns of soil carbon turnover time derived with models. Areas with no biomass (mean annual NDVI below 0.1) are masked with grey.

**Figure S4** Pearson correlation coefficient between MAT (or MAP) and  $\tau_{veg}$  (or  $\tau_{soil}$ ) for all models at grid scale. (a) correlation between MAT and  $\tau_{veg}$ ; (b) correlation between MAT and  $\tau_{soil}$ ; (c) correlation between MAP and  $\tau_{veg}$ ; and (d) correlation between MAP and  $\tau_{soil}$ . Stippling indicates locations where the correlation is significant ( $p < 0.05$ ). Inserted figures represent frequency histogram of corresponding correlation coefficients (r). Percentages of the

significant regions ( $p < 0.05$ ) account for the total applied land area are tagged in the inserted figures.

**Figure S5** Spatial sensitivity of model-based biomass carbon turnover time to temperature (T) in a  $5^{\circ}$  by  $5^{\circ}$  moving window using a multiple linear regression approach. Stippling indicates locations where model-based sensitivity is significant ( $p < 0.05$ ). Areas with no biomass (mean annual NDVI below 0.1) are masked with grey.

**Figure S6** Spatial sensitivity of model-based biomass carbon turnover time to precipitation (P) in a  $5^{\circ}$  by  $5^{\circ}$  moving window using a multiple linear regression approach. Stippling indicates locations where model-based sensitivity is significant ( $p < 0.05$ ). Areas with no biomass (mean annual NDVI below 0.1) are masked with grey.

**Figure S7** Spatial sensitivity of model-based soil carbon turnover time to temperature (T) in a  $5^{\circ}$  by  $5^{\circ}$  moving window using a multiple linear regression approach. Stippling indicates locations where model-based sensitivity is significant ( $p < 0.05$ ). Areas with no biomass (mean annual NDVI below 0.1) are masked with grey.

**Figure S8** Spatial sensitivity of model-based soil carbon turnover time to precipitation (P) in a  $5^{\circ}$  by  $5^{\circ}$  moving window using a multiple linear regression approach. Stippling indicates locations where model-based sensitivity is significant ( $p < 0.05$ ). Areas with no biomass (mean annual NDVI below 0.1) are masked with grey.

**Figure S9** Spatial sensitivity of biomass carbon turnover time to climate (temperature, T and precipitation, P) in a  $7^{\circ}$  by  $7^{\circ}$  moving window using a multiple linear regression approach.

**Figure S10** Spatial sensitivity of soil carbon turnover time to climate (temperature, T and precipitation, P) in a  $7^{\circ}$  by  $7^{\circ}$  moving window using a multiple linear regression approach.

**Figure S11** Spatial sensitivity of biomass carbon turnover time to climate (temperature, T and precipitation, P) in a  $9^{\circ}$  by  $9^{\circ}$  moving window using a multiple linear regression approach.

**Figure S12** Spatial sensitivity of soil carbon turnover time to climate (temperature, T and precipitation, P) in a  $9^{\circ}$  by  $9^{\circ}$  moving window using a multiple linear regression approach.

**Figure S13** Relationships between forest cover and carbon turnover times ( $\tau_{soil}$  and  $\tau_{veg}$ ) in boreal forest (a, b), temperate forest (c, d) and tropical rainforest (e, f). Curves show median values among models, and the filled area represents median absolute deviation. The black line is based on observation data, and others are derived with CMIP5 models which also output forest cover variable.

**Figure S14** Comparison of  $\tau_{veg}$  in tropical rainforest derived with biomass carbon from Liu et al. (2015) and from Saatchi et al. (2011).

**Figure S15** Comparison of global  $\tau_{soil}$  in this study with that based on soil carbon and NPP from Bloom et al. (2016).

**Figure S16** Comparison between NPP and biomass outflux for all of the CMIP5 models.

**Figure S17** Comparison between NPP and soil outflux for all of the CMIP5 models.

**Figure S18** Comparison between  $\tau_{veg}$  and  $\tau_{vegout}$  for all of the CMIP5 models.

**Figure S19** Comparison between  $\tau_{soil}$  and  $\tau_{soilout}$  for all of the CMIP5 models.

**Table S1** Summary of CMIP5 ESMs used in this study, including model name, coupled atmosphere model, coupled land model, nitrogen cycle (N), land use change (LUC) and fire.

Model Name	Atmosphere	Land	N	LUC	Fire
BCC_CSM1.1(m)	BCC_AGCM2.1	BCC-AVIM1.0	No	No	No
BNU-ESM	CAM3.5	CoLM+B-NUDGVM	No	Yes	No
CanESM2	CanAM4	CLASS 2.7; CTEM	No	Yes	No
CCSM4	CAM4	CLM4	Yes	Yes	Yes
CESM1(BGC)	CAM4	CLM4	Yes	Yes	Yes
CESM1(CAM5)	CAM5	CLM4	Yes	Yes	Yes
CESM1(WACCM)	WACCM4	CLM4	Yes	Yes	Yes
IPSL-CM5A-LR	LMDZ5	ORCHIDEE	No	Yes	Yes
IPSL-CM5B-LR	LMDZ5	ORCHIDEE	No	Yes	Yes
MIROC-ESM-CHEM	MIROC-AGCM	MATSIRO	No	Yes	No
MPI-ESM-LR	ECHAM6	JSBACH	No	Yes	Yes
MPI-ESM-MR	ECHAM6	JSBACH	No	Yes	Yes
MRI-ESM1	MRI-AGCM3.3	HAL	No	No	No
NorESM1-ME	CAM4-Oslo	CLM4	Yes	Yes	Yes

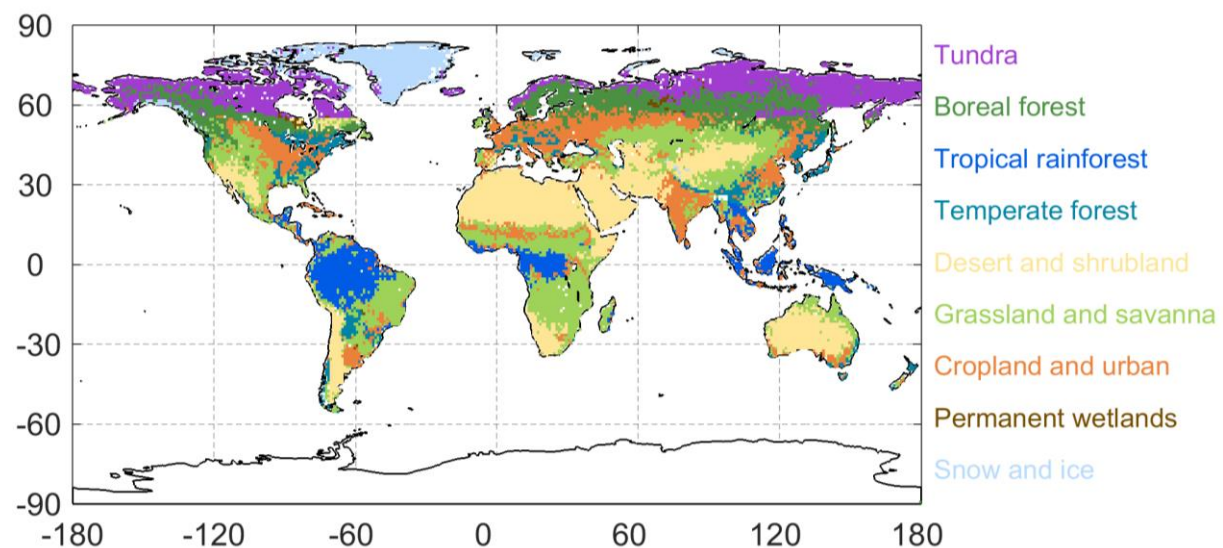


**Figure S1** Global biome map constructed from the Moderate Resolution Imaging Spectroradiometer (MODIS) International Geosphere-Biosphere Program (IGBP) land-cover map referred to Todd-Brown et al. (2013).

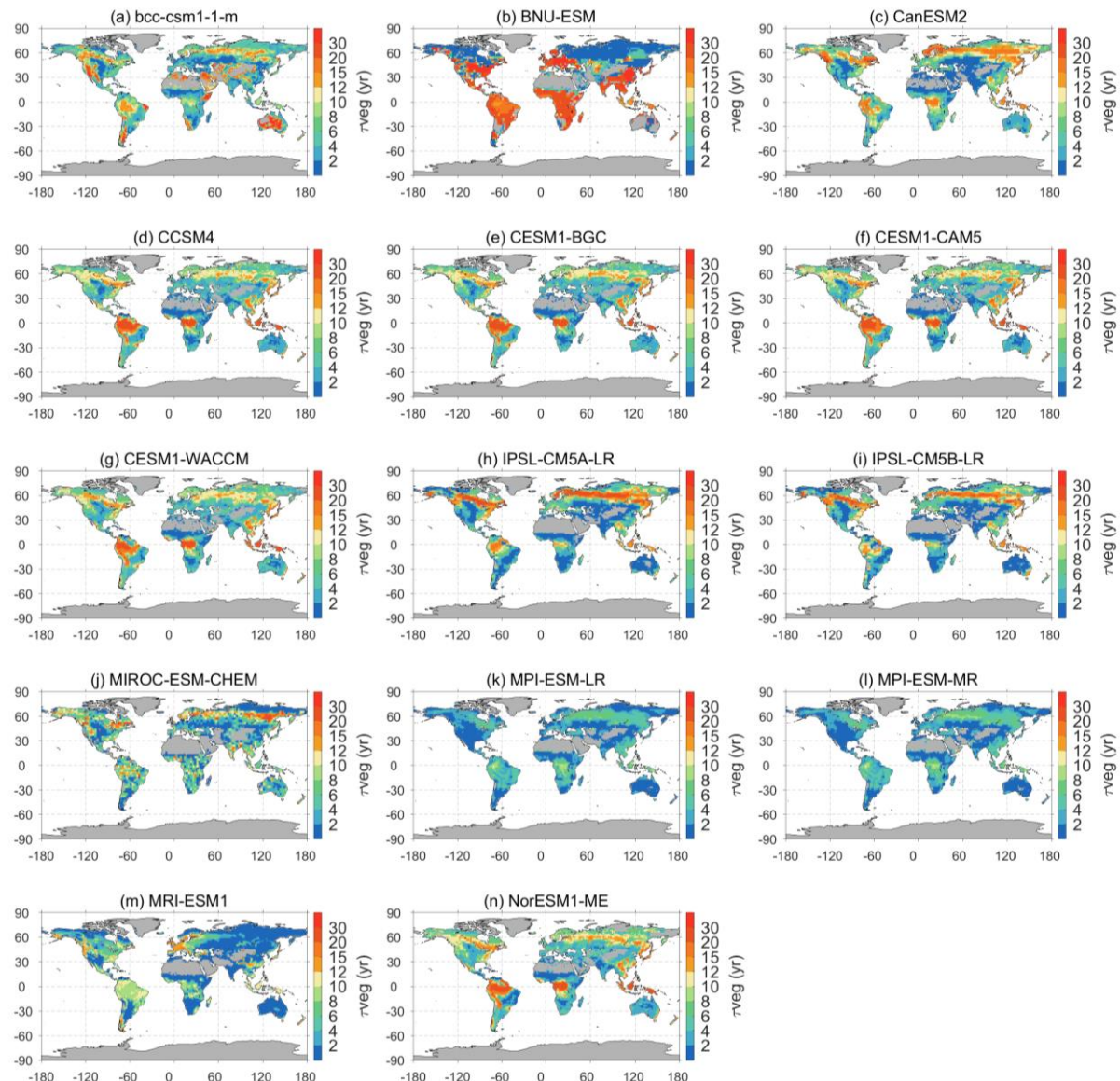


**Figure S2** Spatial patterns of biomass carbon turnover time derived with models. Areas with no biomass (mean annual NDVI below 0.1) are masked with grey.

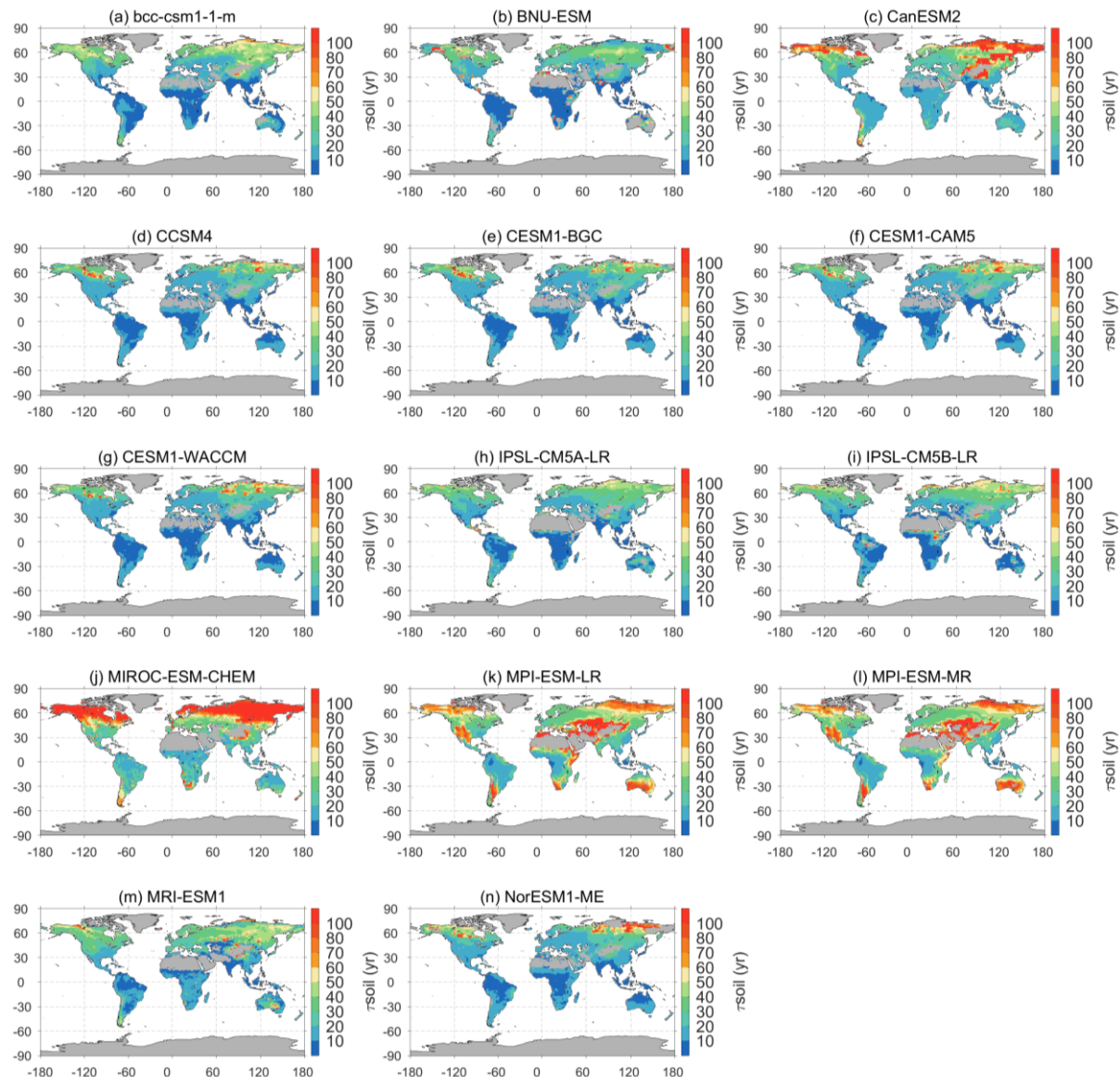


**Figure S3** Spatial patterns of soil carbon turnover time derived with models. Areas with no biomass (mean annual NDVI below 0.1) are masked with grey.

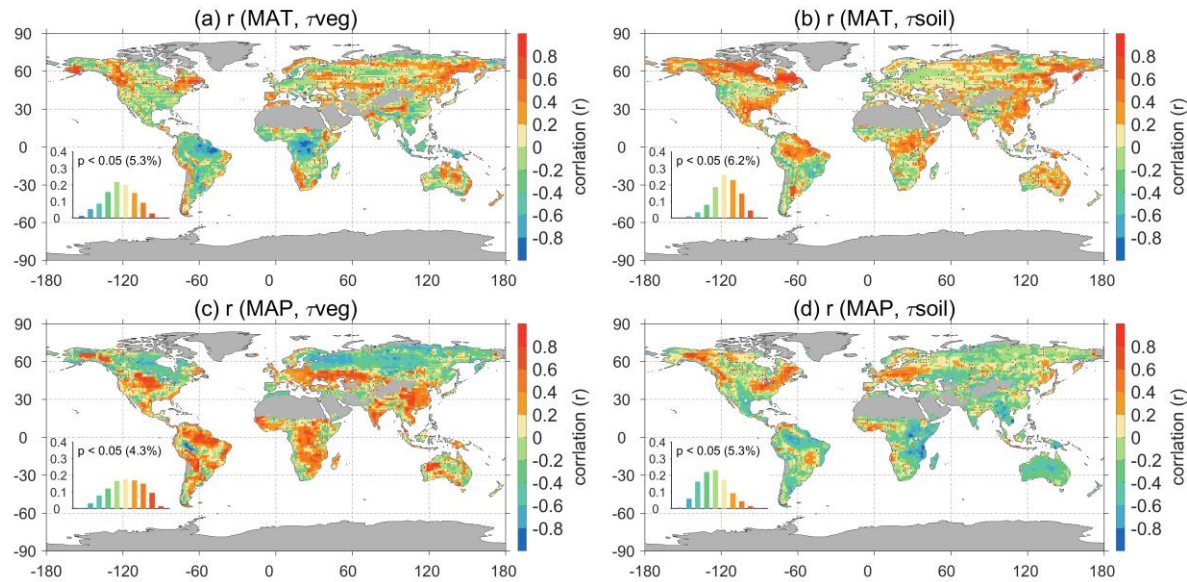


**Figure S4** Pearson correlation coefficient between MAT (or MAP) and  $\tau_{veg}$  (or  $\tau_{soil}$ ) for all models at grid scale. (a) correlation between MAT and  $\tau_{veg}$ ; (b) correlation between MAT and  $\tau_{soil}$ ; (c) correlation between MAP and  $\tau_{veg}$ ; and (d) correlation between MAP and  $\tau_{soil}$ . Stippling indicates locations where the correlation is significant ( $p < 0.05$ ). Inserted figures represent frequency histogram of corresponding correlation coefficients ( $r$ ). Percentages of the significant regions ( $p < 0.05$ ) account for the total applied land area are tagged in the inserted figures.

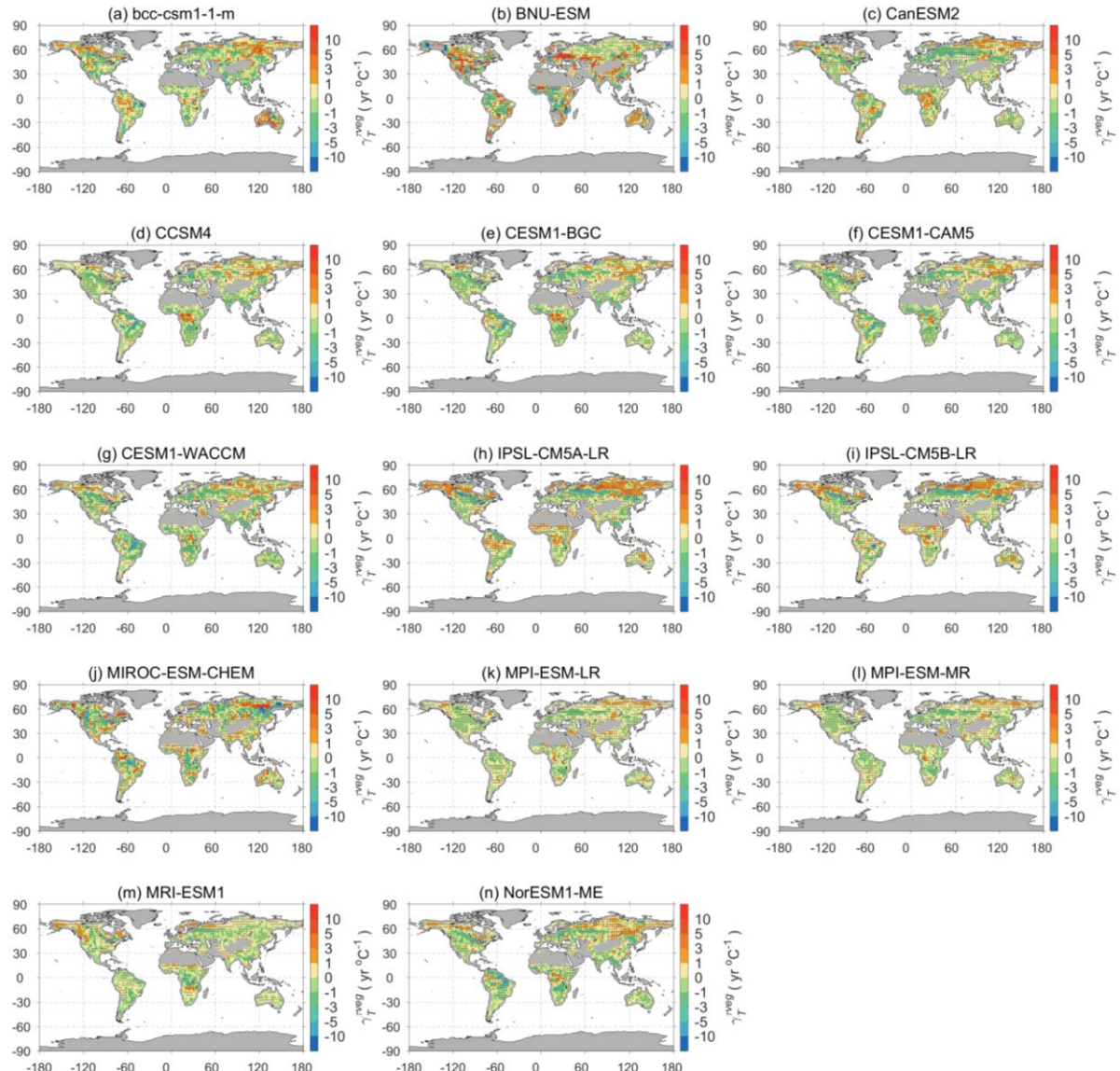


**Figure S5** Spatial sensitivity of model-based biomass carbon turnover time to temperature (T)

in a  $5^{\circ}$  by  $5^{\circ}$  moving window using a multiple linear regression approach. Stippling indicates locations where model-based sensitivity is significant ( $p < 0.05$ ). Areas with no biomass (mean annual NDVI below 0.1) are masked with grey.

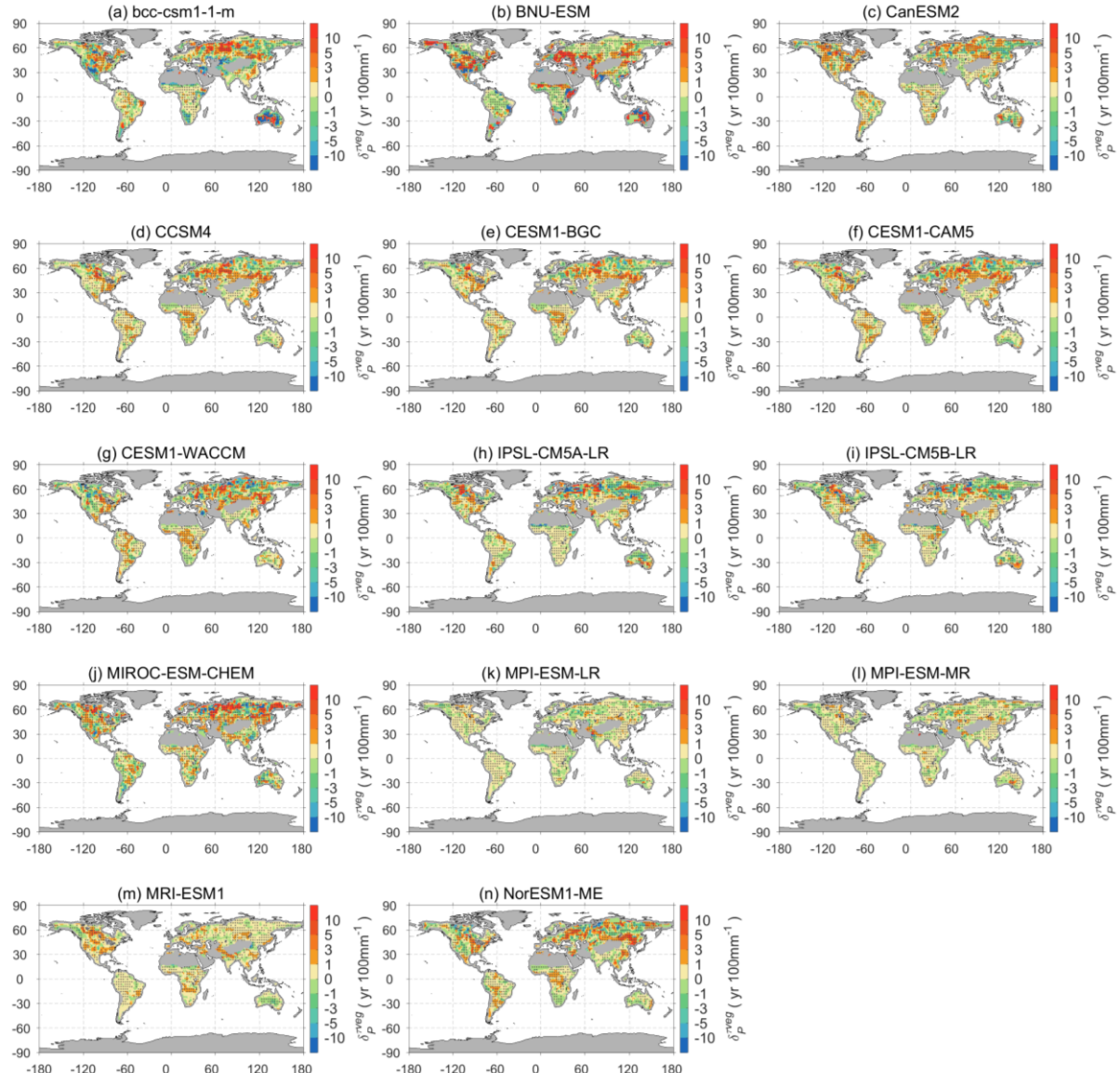


**Figure S6** Spatial sensitivity of model-based biomass carbon turnover time to precipitation (P)

in a  $5^{\circ}$  by  $5^{\circ}$  moving window using a multiple linear regression approach. Stippling indicates locations where model-based sensitivity is significant ( $p < 0.05$ ). Areas with no biomass (mean annual NDVI below 0.1) are masked with grey.

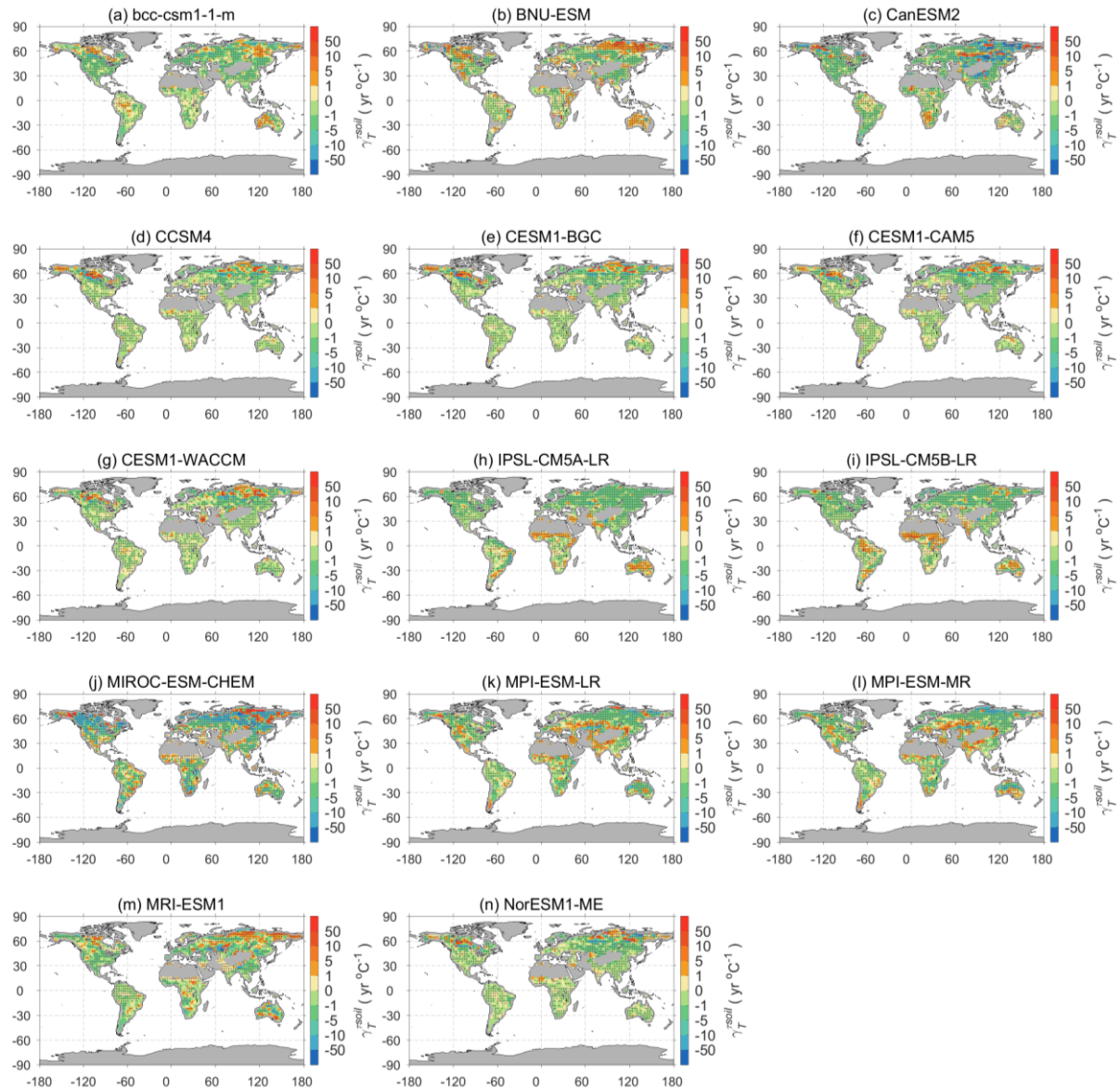


**Figure S7** Spatial sensitivity of model-based soil carbon turnover time ( $T$ ) in a  $5^\circ$  by  $5^\circ$  moving window using a multiple linear regression approach. Stippling indicates locations where model-based sensitivity is significant ( $p < 0.05$ ). Areas with no biomass (mean annual NDVI below 0.1) are masked with grey.

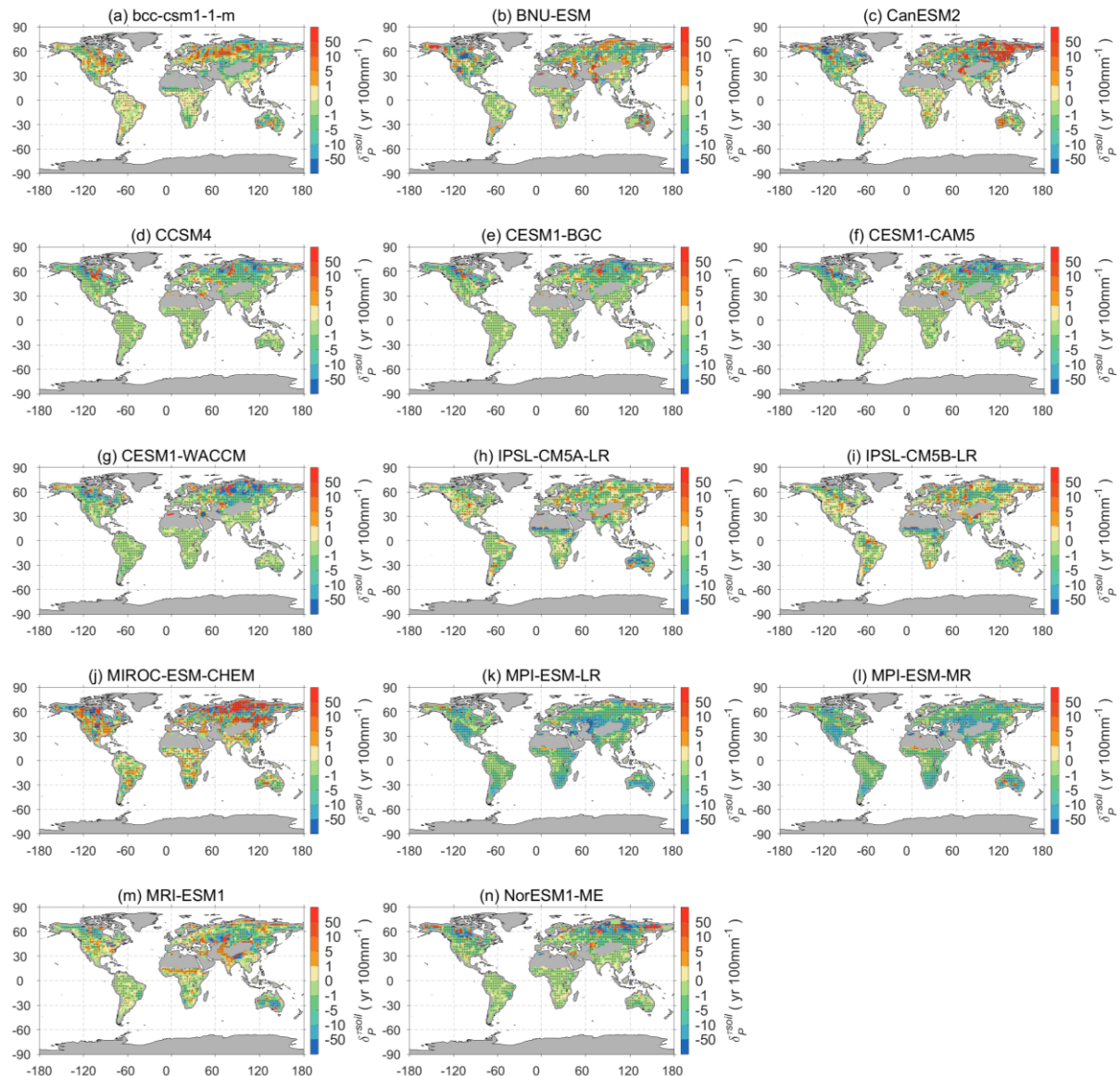


**Figure S8** Spatial sensitivity of model-based soil carbon turnover time to precipitation (P) in a  $5^{\circ}$  by  $5^{\circ}$  moving window using a multiple linear regression approach. Stippling indicates locations where model-based sensitivity is significant ( $p < 0.05$ ). Areas with no biomass (mean annual NDVI below 0.1) are masked with grey.

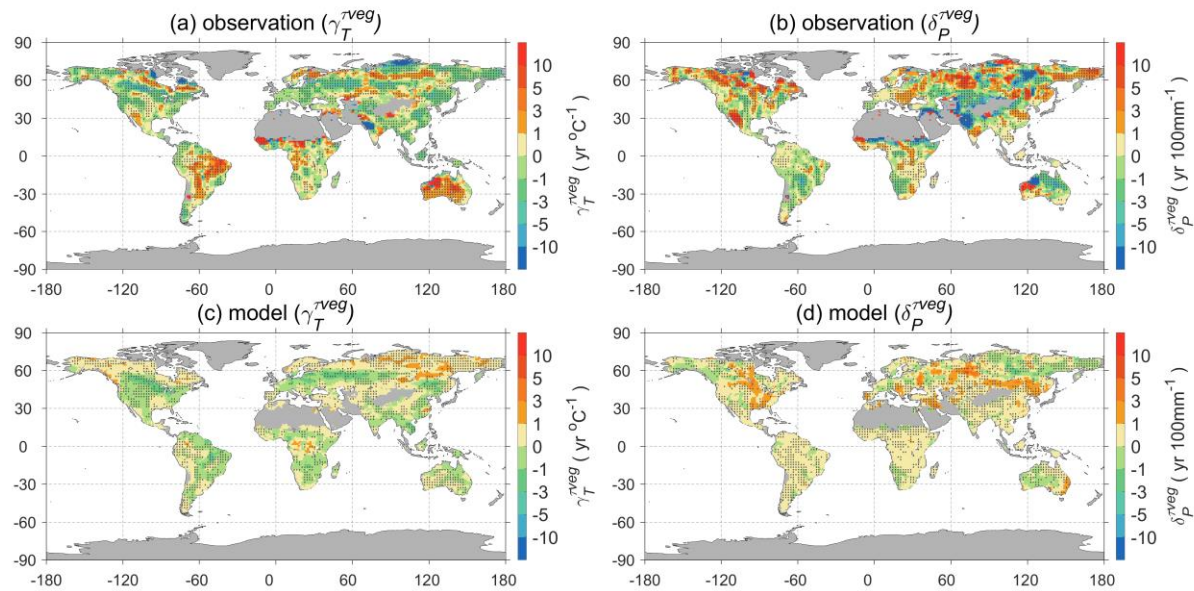


**Figure S9** Spatial sensitivity of biomass carbon turnover time to climate (temperature, T and precipitation, P) in a  $7^\circ$  by  $7^\circ$  moving window using a multiple linear regression approach. (a), and (b) show sensitivity of observation-based biomass carbon turnover time to temperature and precipitation respectively; (c), and (d) show median sensitivity of model-based biomass carbon turnover times to temperature and precipitation respectively. In (a) and (b), stippling indicates locations where observation-based sensitivity is significant ( $p < 0.05$ ); in (c) and (d), stippling indicates where fewer than one quarter of the models are within the 5<sup>th</sup> and 95<sup>th</sup> uncertainty range of the observed sensitivity. Areas with no biomass (mean annual NDVI below 0.1) are masked with grey.

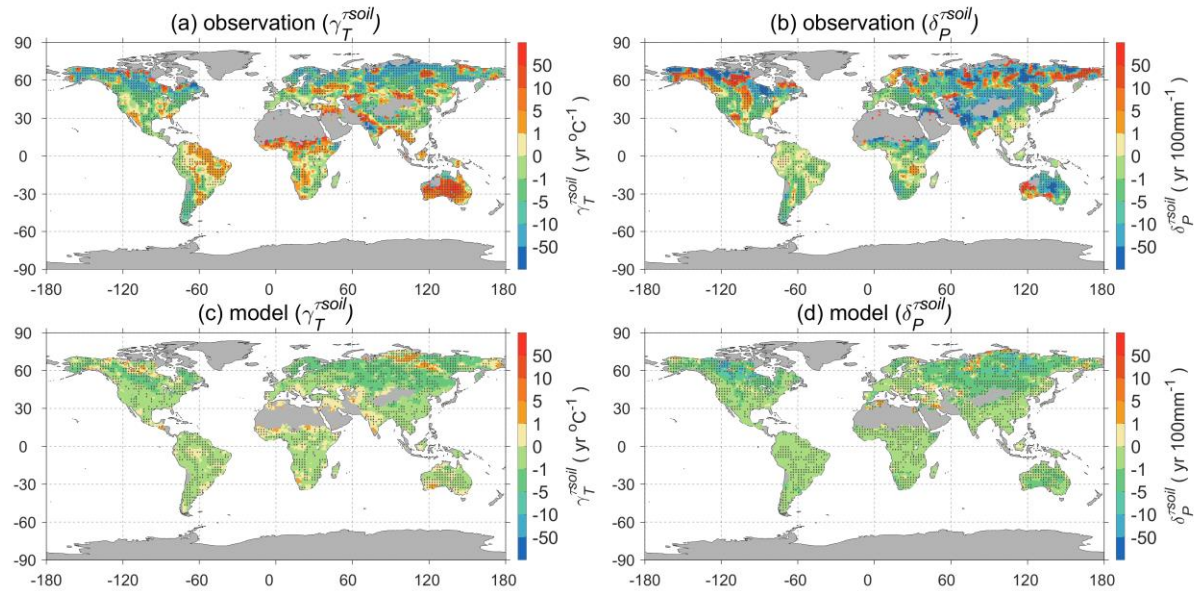


**Figure S10** Spatial sensitivity of soil carbon turnover time to climate (temperature, T and precipitation, P) in a  $7^\circ$  by  $7^\circ$  moving window using a multiple linear regression approach. (a), and (b) show sensitivity of observation-based soil carbon turnover time to temperature and precipitation respectively; (c), and (d) show median sensitivity of model-based soil carbon turnover times to temperature and precipitation respectively. In (a) and (b), stippling indicates locations where observation-based sensitivity is significant ( $p < 0.05$ ); in (c) and (d), stippling indicates where fewer than one quarter of the models are within the 5<sup>th</sup> and 95<sup>th</sup> uncertainty range of the observed sensitivity. Areas with no biomass (mean annual NDVI below 0.1) and data are masked with grey.

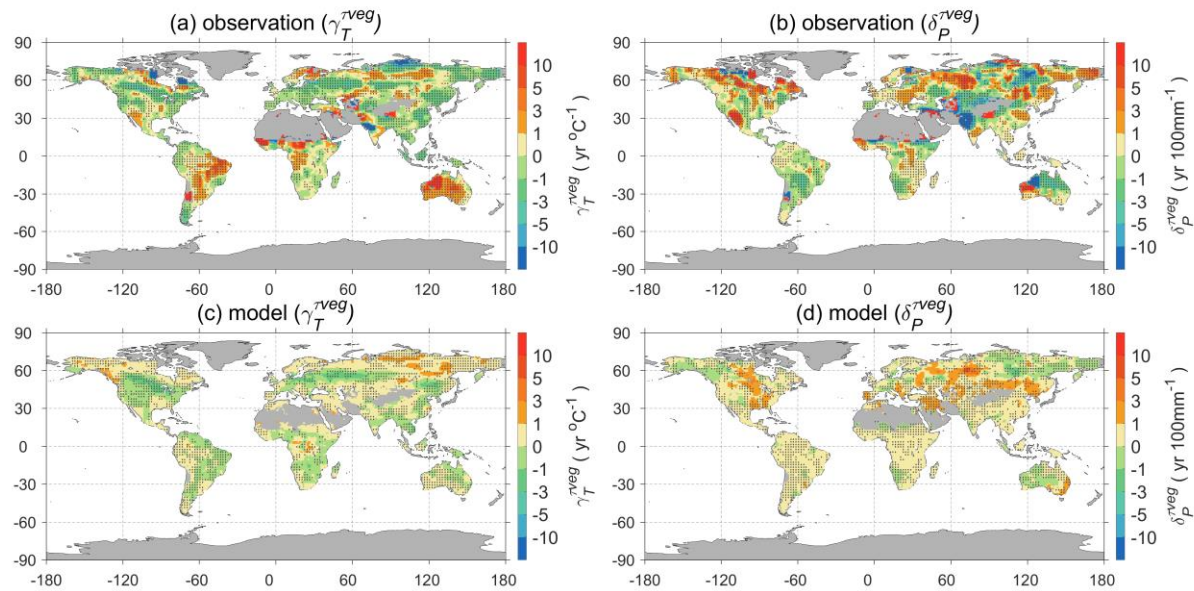


**Figure S11** Spatial sensitivity of biomass carbon turnover time to climate (temperature, T and precipitation, P) in a  $9^\circ$  by  $9^\circ$  moving window using a multiple linear regression approach. (a), and (b) show sensitivity of observation-based biomass carbon turnover time to temperature and precipitation respectively; (c), and (d) show median sensitivity of model-based biomass carbon turnover times to temperature and precipitation respectively. In (a) and (b), stippling indicates locations where observation-based sensitivity is significant ( $p < 0.05$ ); in (c) and (d), stippling indicates where fewer than one quarter of the models are within the 5<sup>th</sup> and 95<sup>th</sup> uncertainty range of the observed sensitivity. Areas with no biomass (mean annual NDVI below 0.1) are masked with grey.

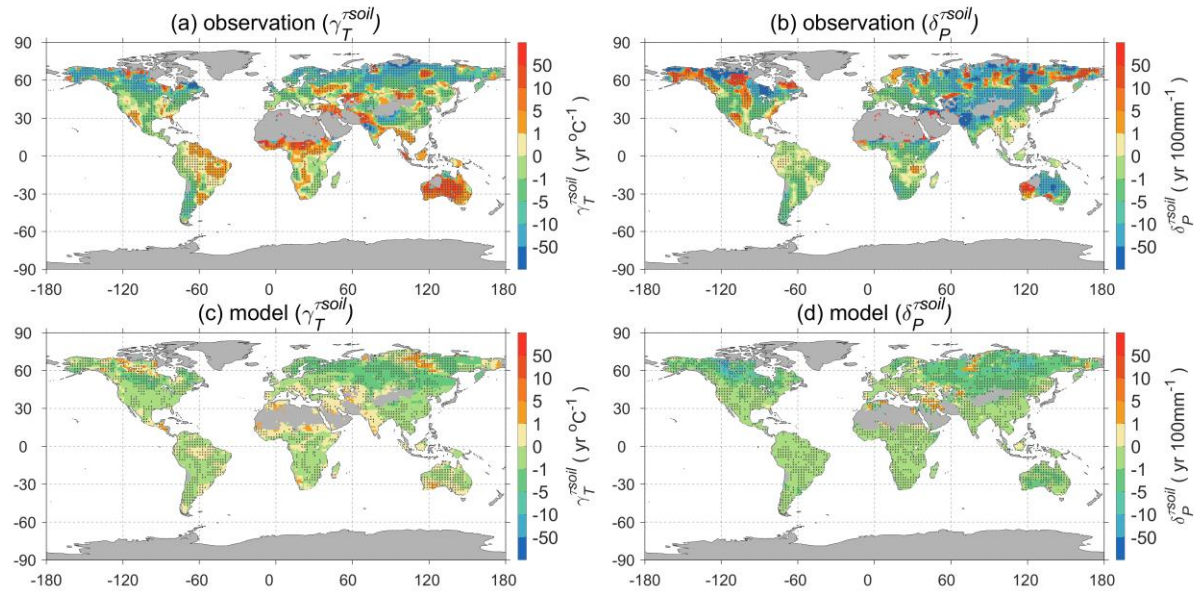


**Figure S12** Spatial sensitivity of soil carbon turnover time to climate (temperature, T and precipitation, P) in a 9° by 9° moving window using a multiple linear regression approach. (a), and (b) show sensitivity of observation-based soil carbon turnover time to temperature and precipitation respectively; (c), and (d) show median sensitivity of model-based soil carbon turnover times to temperature and precipitation respectively. In (a) and (b), stippling indicates locations where observation-based sensitivity is significant ( $p < 0.05$ ); in (c) and (d), stippling indicates where fewer than one quarter of the models are within the 5<sup>th</sup> and 95<sup>th</sup> uncertainty range of the observed sensitivity. Areas with no biomass (mean annual NDVI below 0.1) and data are masked with grey.

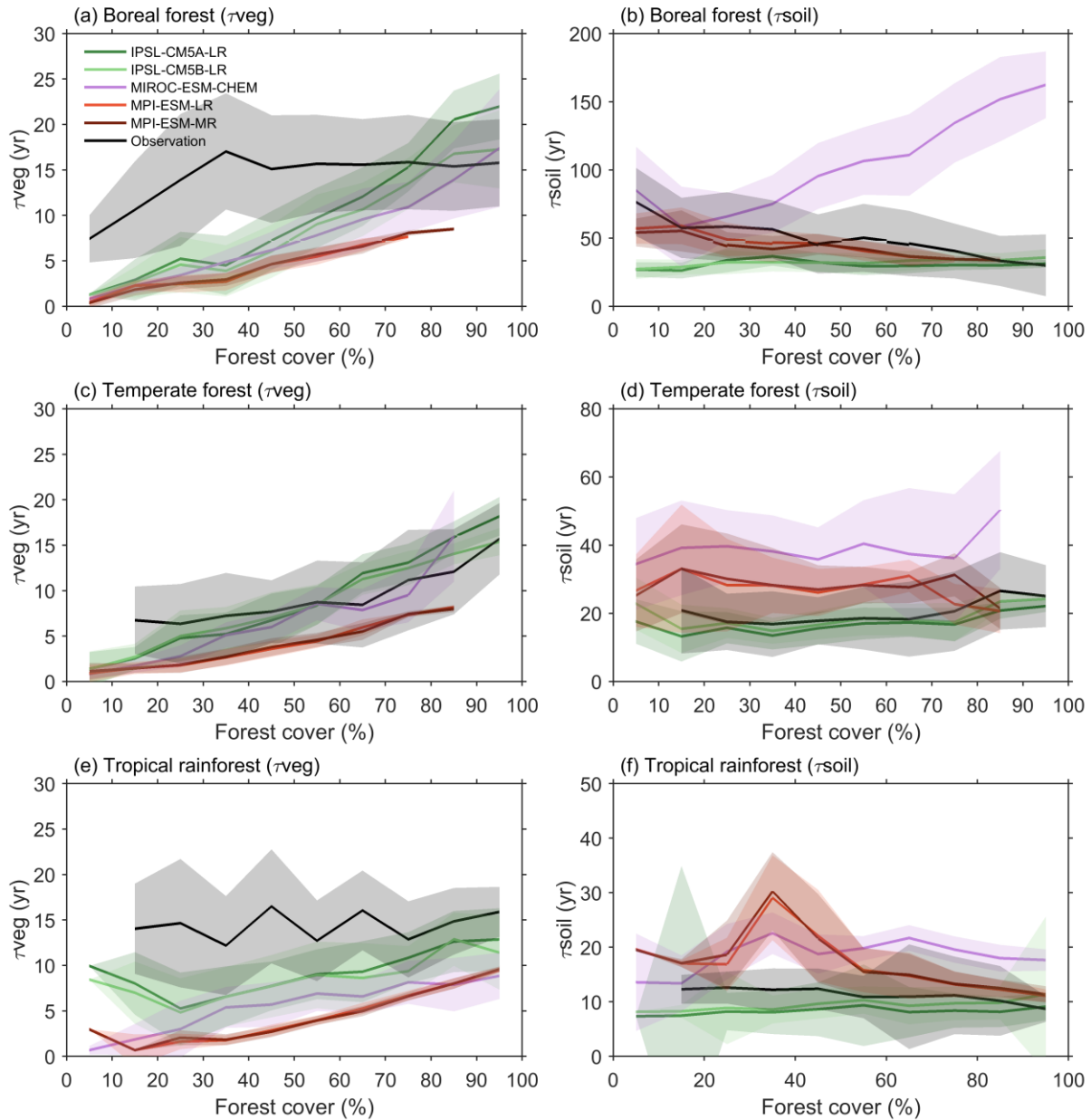


**Figure S13** Relationships between forest cover and carbon turnover times ( $\tau_{soil}$  and  $\tau_{veg}$ ) in boreal forest (a, b), temperate forest (c, d) and tropical rainforest (e, f). Curves show median values among models, and the filled area represents median absolute deviation. The black line is based on observation data, and others are derived with CMIP5 models which also output forest cover variable.

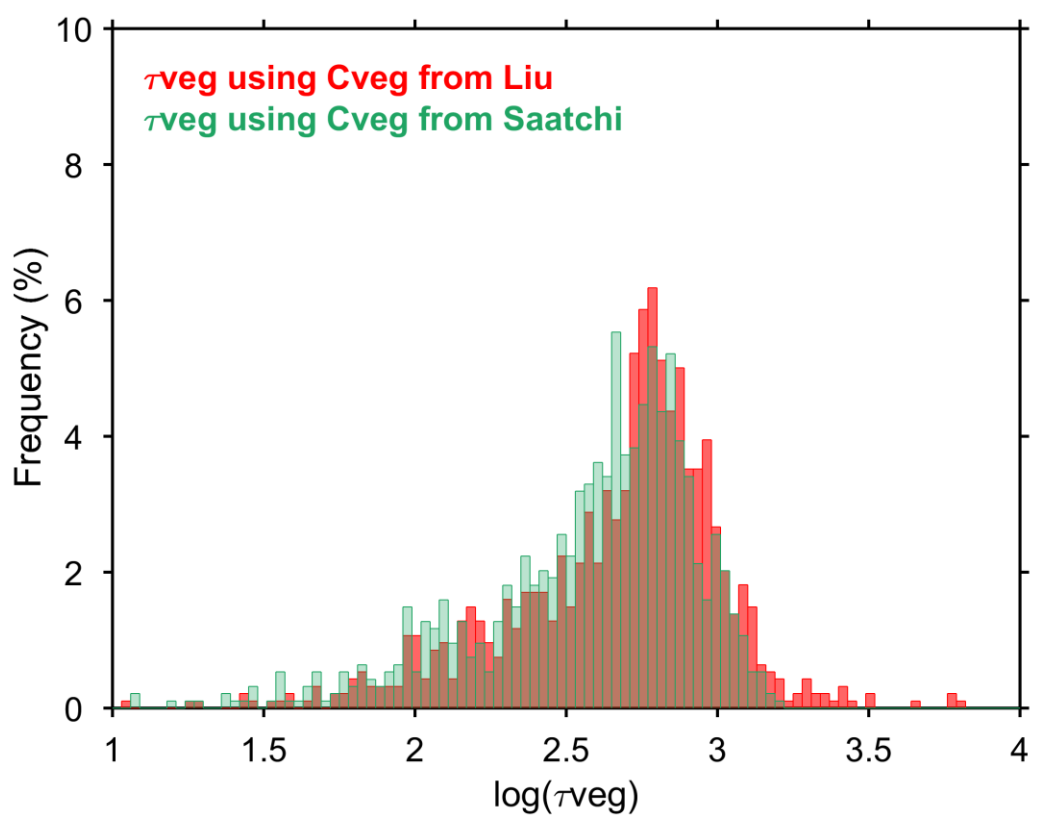


**Figure S14** Comparison of  $\tau_{veg}$  in tropical rainforest derived with biomass carbon from Liu et al. (2015) and from Saatchi et al. (2011).

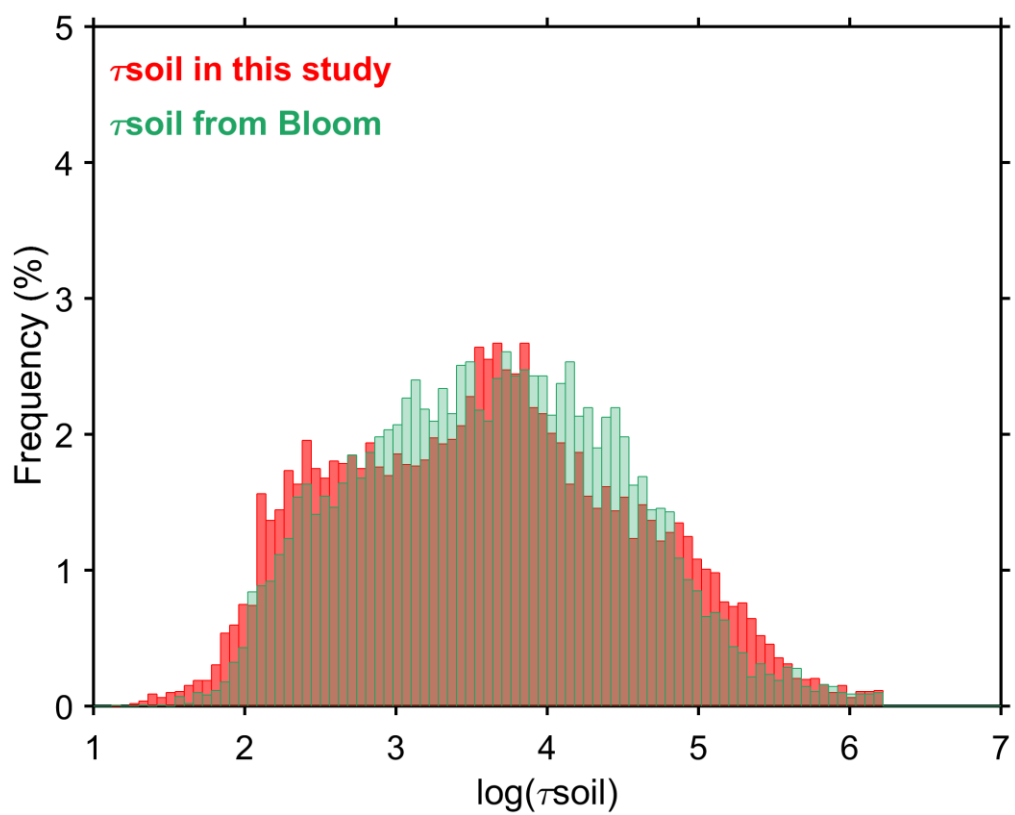


**Figure S15** Comparison of global  $\tau_{\text{soil}}$  in this study with that based on soil carbon and NPP from Bloom et al. (2016).

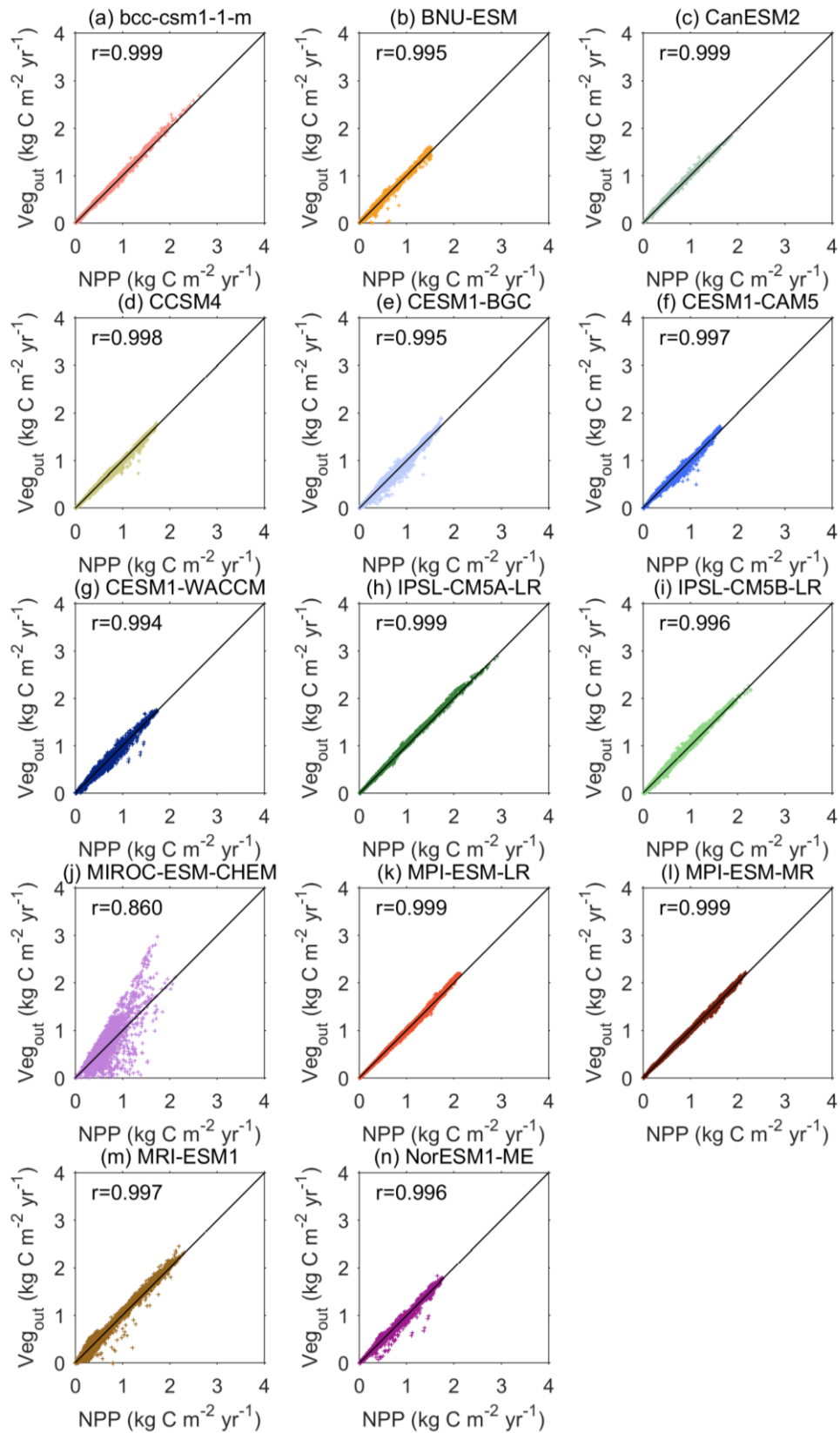


**Figure S16** Comparison between NPP and biomass outflux for all of the CMIP5 models.

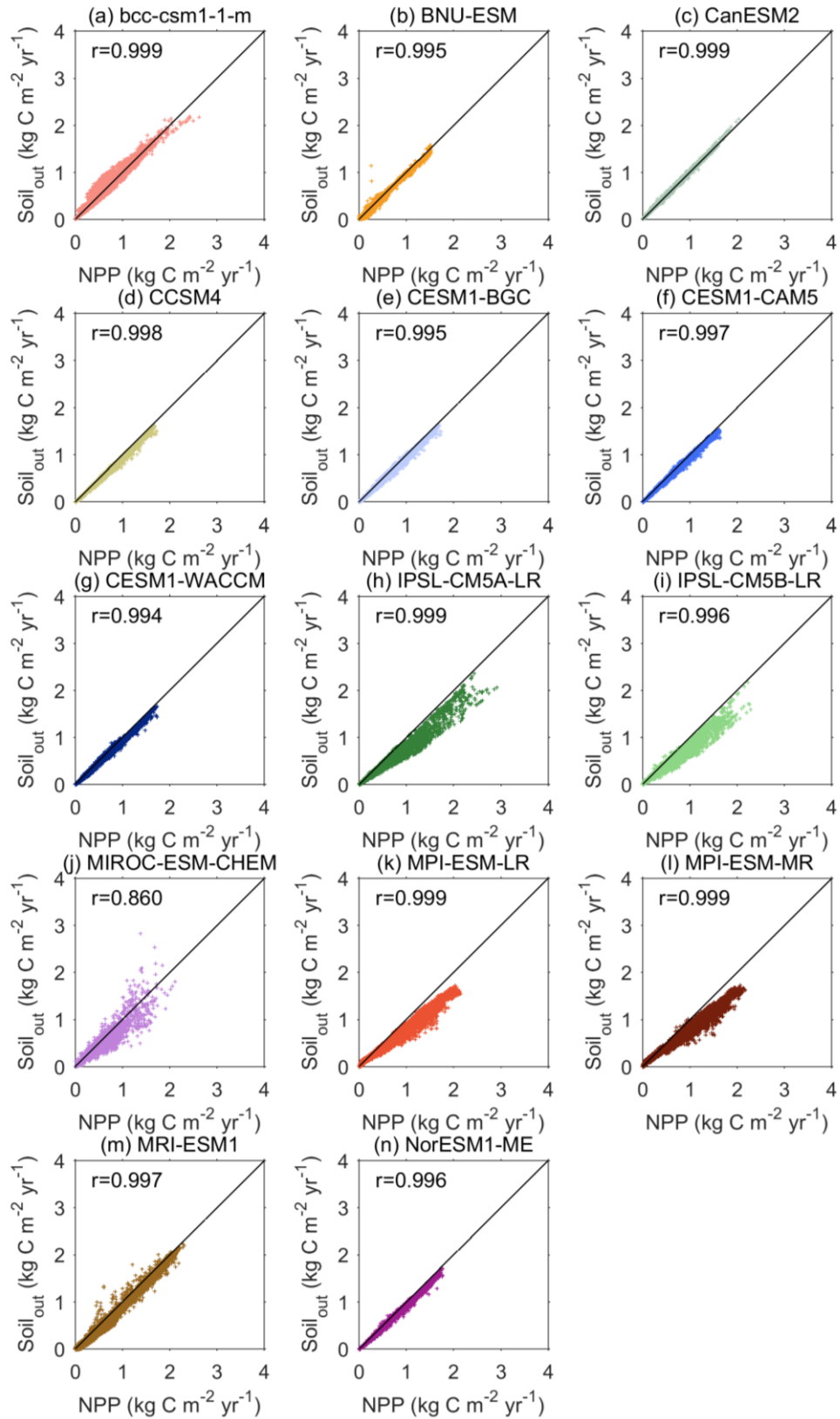


**Figure S17** Comparison between NPP and soil outflux for all of the CMIP5 models.

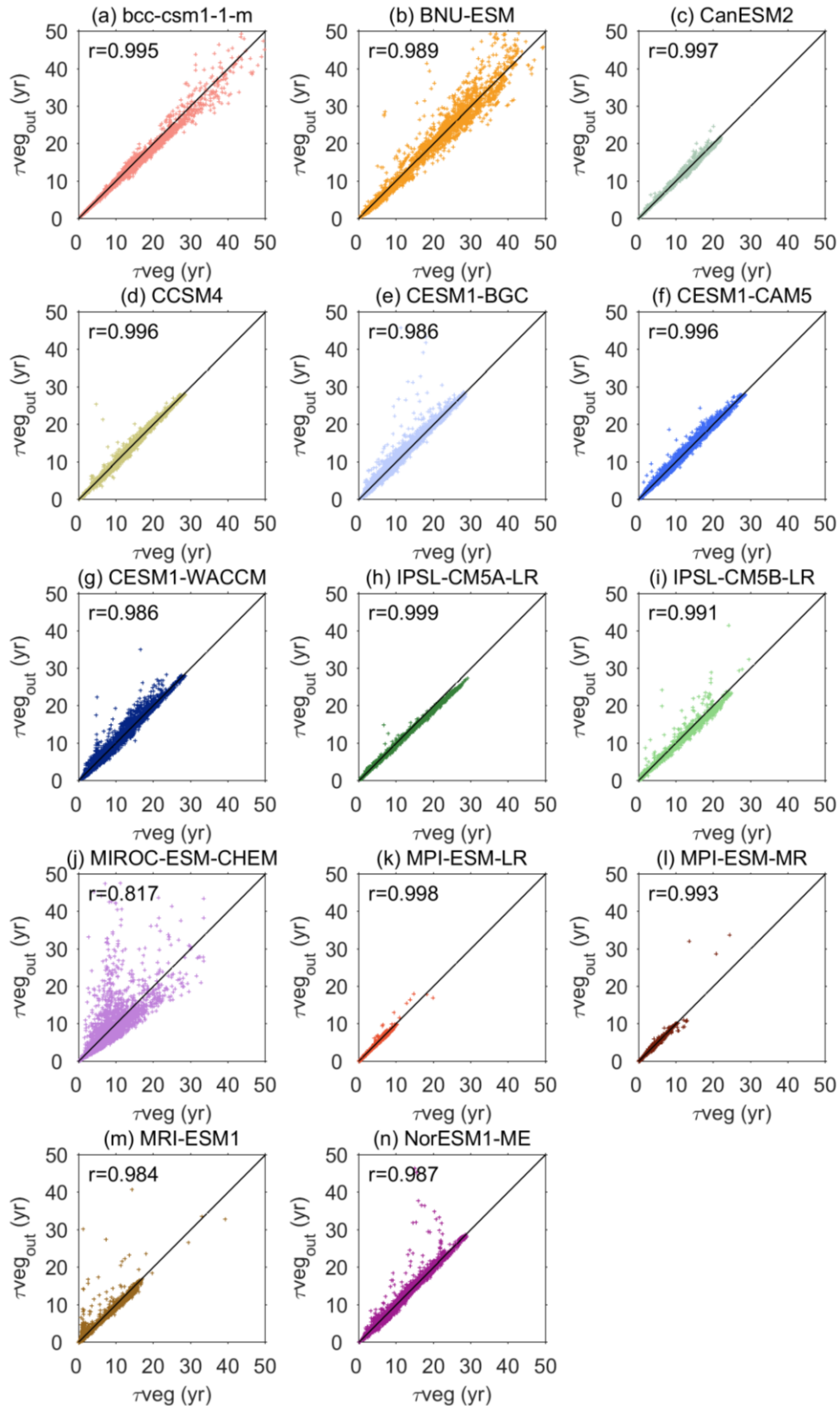


**Figure S18** Comparison between  $\tau_{veg}$  and  $\tau_{vegout}$  for all of the CMIP5 models.

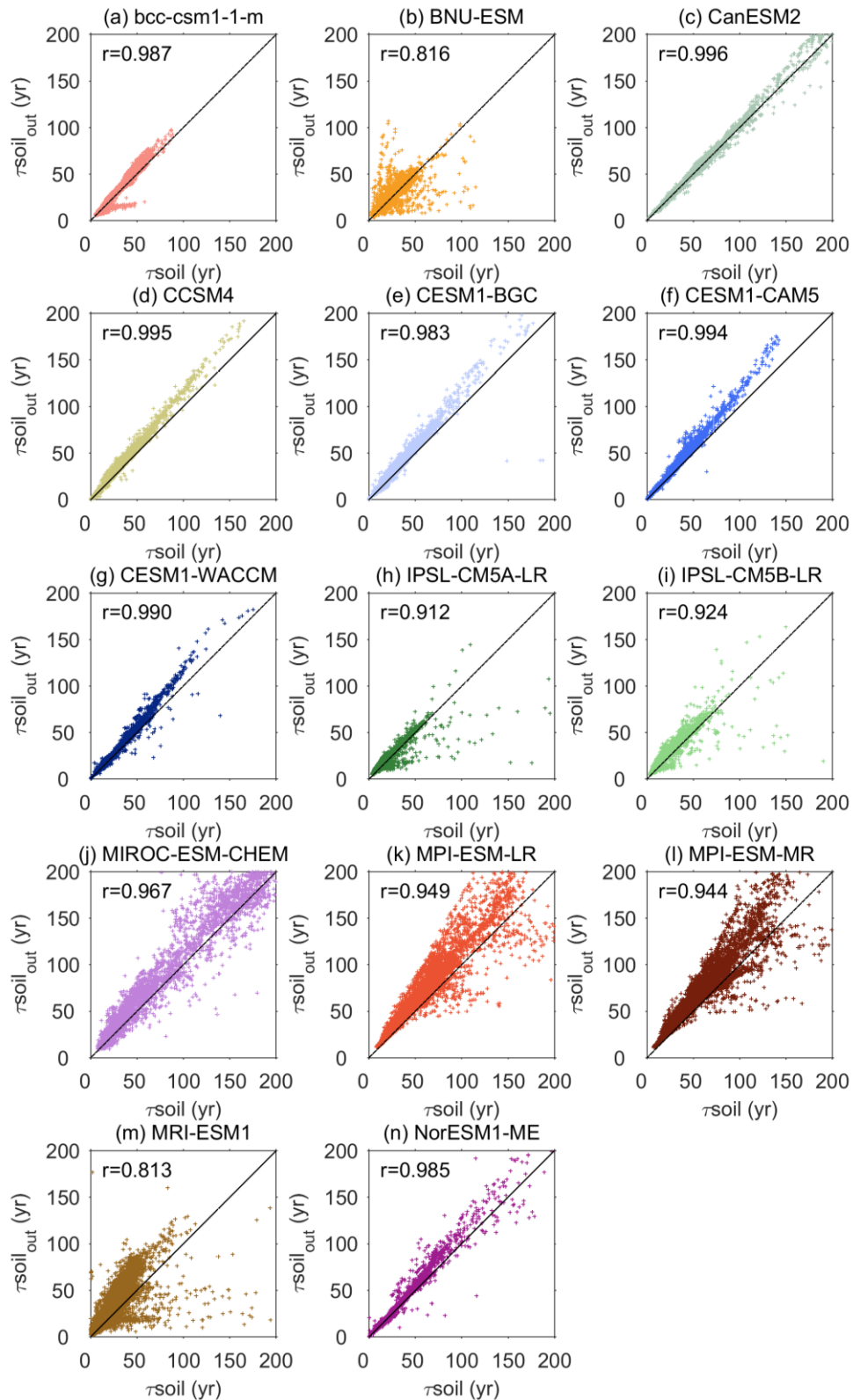


**Figure S19** Comparison between  $\tau_{soil}$  and  $\tau_{soilout}$  for all of the CMIP5 models.